Appl. Math. and Comp. Sci., 1995, vol.5, No.1, 61–88

COMPENSATOR DESIGN FOR THE KIRCHOFF PLATE MODEL WITH BOUNDARY CONTROL[†]

ERIK HENDRICKSON*

This paper presents a compensator design problem in optimal control theory. An algorithm is developed to compute a finite-dimensional compensator based on the Kalman filter theory. The algorithm is implemented using a standard finite element scheme applied to a Kirchoff plate model with boundary control and boundary observation. Convergence of feedback and compensator gains is examined.

1. Introduction

This paper considers a performance optimization problem in control theory and the design of an optimal feedback control law when only partial observation of the state is available. The state dynamics and observation may be subject to sensor noise and disturbances. The standard approach involves the construction of a dynamical observer which is based only upon the information available through the observation. The optimal control law, called the compensator, is based on the observer (estimate) and produces optimal performance of the resulting closed-loop system. One of the difficulties of this problem, aside from the nature of the control (applied on the boundary) is that the original system is infinite dimensional. But practicality requires both the estimate and the compensator be finite dimensional. Hence, the main goal is to develop an algorithm that constructs a finite-dimensional compensator that produces near optimal performance when applied to the original dynamics. The algorithm includes a regularization of the original problem and an approximation of the regularized problem. The regularization is necessary to ensure that critical approximation assumptions are satisfied by the chosen numerical scheme.

The numerical work expands upon the recent theory in (Hendrickson, 1994; Hendrickson and Lasiecka, 1993; Lasiecka, 1992) and examines the effect of various design parameters on the compensator design process. The main goals of the paper are twofold, (i) to assert numerical validity of the theoretical results predicted by the theory presented in (Hendrickson, 1994), (ii) to examine the effect of various parameters entering the design process with respect to the accuracy of the predicted results. The emphasis of the investigation is divided into two parts which arise naturally due to the the separation principle. First we examine the feedback gain and the associated closed-loop system arising in the deterministic control problem. We

[†] This research was partially supported by the Laboratory of Scientific Computing, University of Jyvaskyla, Finland, directed by Prof. Pekka Neittaanmaki.

* Institute of Applied Mathematics, University of Virginia, Charlottesville, Virginia, 22901

observe the effects of varying the weights in the cost functional as well as the effects of the interior and boundary regularization terms. Convergence of the feedback gains is examined as well as stabilization properties of the closed-loop system. Secondly, we examine the estimator gain and the decay of the error between the estimated and full state. We also consider the effects that the covariances of the noise processes have on the decay rate of the estimation error.

2. Formulation of Problem

We consider the following system,

$$\begin{aligned} & kw_{tt} - \gamma \Delta w_{tt} + \Delta^2 w = 0 \quad \text{on} \quad \Omega \times (0,\infty) \\ & w(x,t) = 0 \quad \text{on} \quad \Gamma \\ & \Delta w(x,t) = 0 \quad \text{on} \quad \Gamma_0 \times (0,\infty) \\ & \Delta w(x,t) = u(t) \quad \text{on} \quad \Gamma_1 \times (0,\infty), \quad \Gamma_0 \bigcup \Gamma_1 \equiv \Gamma \\ & w(x,0) = w_0(x), \quad w_t(x,0) = w_1(x) \quad \text{on} \quad \Omega \end{aligned} \tag{1}$$

with boundary observation

$$z(t) = C(w, w_t) = \frac{\partial}{\partial \nu} w(x,t) \quad \text{on} \quad \Gamma_1 \times (0,\infty) \tag{2}$$

The variable $w(x,t)$ represents the vertical displacement of the plate, $u(t)$ acts as a boundary control in the form of a bending moment, k pertains to the flexibility of the plate, $\gamma > 0$ is a parameter that is proportional to the plate thickness, and the only observation is the normal derivative at the left endpoint. Notice that the uncontrolled $(u(t) = 0)$ is unstable, i.e. there are infinitely many eigenvalues on the imaginary axis. Hence, the selected boundary control must not only stabilize the system but also be based on the available information from the boundary observation and be finite-dimensional.

With (1) we associate the quadratic cost functional (performance index),

$$J\Big(u, w(u)\Big) = \int_0^\infty \Big(\|Qw\|_H^2 \; + \; \|Ru\|_{L_2(\Gamma)}^2 \Big) \, \mathrm{d}t \tag{3}$$

The combination of system (1) with the performance index (3) represents a regulator problem, in which the goal is to return the system to its zero state in an optimal fashion, or in a sense, track the desired zero state trajectory.

The control problem (3) can be placed into the following abstract framework

$$x \equiv (w, w_t), \qquad R \in \mathcal{L}\Big(L_2(\Gamma)\Big), \qquad Q \in \mathcal{L}(H)$$

where Hilbert spaces H, U, Z are defined as

$$H \equiv H^2(\Omega) \cap H_0^1(\Omega) \times H_0^1(\Omega), \qquad U = L_2(\Gamma), \qquad Z = L_2(\Gamma)$$

$\mathcal{H} \equiv H_0^1(\Omega)$ has inner product defined as $(u,v)_{\mathcal{H}} = \displaystyle\int_\Omega uv \, \mathrm{d}\Omega + \gamma \int_\Omega \nabla u \nabla v \, \mathrm{d}\Omega$

We can express the energy of the system as

$$E(t) = \int_\Omega |\Delta w(t)|^2 + \gamma |\nabla w_t|^2 + |w_t|^2 \, d\Omega$$

and define the H-norm as the energy of the system, i.e.

$$\|x\|_H^2 = E(x,t)$$

$$A \equiv \begin{bmatrix} 0 & I \\ -\mathcal{A} & 0 \end{bmatrix}, \qquad \mathcal{D}(A) \equiv \mathcal{D}(\mathcal{A}) \times \mathcal{H}, \quad \text{and} \quad B \equiv \begin{bmatrix} 0 \\ \mathcal{B} \end{bmatrix}$$

$$A_D y \equiv \Delta y; \quad \mathcal{D}(A_D) \equiv \Big(y \in H^2(\Omega); \; y|_\Gamma = 0 \Big)$$

$$\mathcal{A} : \mathcal{H} \to \mathcal{H}; \quad \mathcal{A} \equiv (I + \gamma A_D)^{-1} {A_D}^2$$

$$\mathcal{B} \equiv (I + \gamma A_D)^{-1} A_D D$$

The Dirichlet map D, $D \in \mathcal{L}\big(H^s(\Gamma) \to H^{s+1/2}(\Omega)\big)$, for any real s, is defined by

$$Du \equiv g \iff \Delta g = 0 \text{ in } \Omega; \; g|_\Gamma = u$$

Notice that on $\mathcal{D}(A_D)$, $\mathcal{A}$ acts as a bounded perturbation of $\frac{1}{\gamma} A_D$, which shows the hyperbolic nature of the system (Lasiecka and Triggiani, 1991b). The operator B satisfies (Lasiecka and Triggiani, 1991a) the following trace hypothesis

$$\int_0^T \|B^* e^{A^* t} x\|_U^2 dt \le C_T \|x\|_H^2, \qquad x \in \mathcal{D}(A^*) \tag{4}$$

Hence, the Kirchoff plate model with full state observation can be written in a semigroup form

$$x_t = Ax + Bu \quad \text{on} \quad [\mathcal{D}(A^*)]' \tag{5}$$

Remark 1. The operators A and B (with B unbounded from $U \to H$) are stabilizable and satisfy a "trace" assumption (Lasiecka and Triggiani, 1991a). A complete LQR theory for the continuous Kirchoff model is available in (Lasiecka and Triggiani, 1991a).

Since only the normal derivative of the displacement at Γ_1 in (1) and (2) is known, we design a dynamic observer that will reconstruct the full state such that the error between the full and estimated states decays exponentially to zero. This design can be subject to conditions such as optimality requirements or desired decay rates. The estimator has the form

$$\dot{\hat{x}}(t) = A\hat{x}(t) + Bu(t) + K(z(t) - C\hat{x}(t)) = (A - KC)\hat{x}(t) + Bu(t) + Kz(t) \tag{6}$$

We choose the feedback law F and the compensator gain K such that

$$F \equiv -B^*P \tag{7}$$

$$K \equiv \hat{P}C^* \tag{8}$$

where P, $\hat{P} \in \mathcal{L}(H)$ are the solutions to the following algebraic Riccati equations,

$$(A^*Px, y)_H + (PAx, y)_H - (B^*Px, B^*Py)_U + (Q^*Qx, y)_H = 0 \tag{9}$$

$$(A\hat{P}x, y)_H + (\hat{P}A^*x, y)_H - (C\hat{P}x, C\hat{P}y)_Z + (\hat{Q}^*\hat{Q}x, y)_H = 0 \tag{10}$$

where $\hat{Q}$, $\hat{R} \in \mathcal{L}(H)$. The theory of existence and uniqueness of solutions to algebraic Riccati equations with *unbounded* control operators (such as B in our problem) has been given in (Flandoli *et al.*, 1988). In fact, it has been shown that equations (9) and (10) are uniquely solvable provided that the following conditions, in addition to the trace hypothesis (4), hold true,

$$(A^*, C^*), \ (A, B) \quad \text{are stabilizable on } H \tag{11}$$

$$(A^*, \hat{Q}), \ (A, Q) \quad \text{are detectable on } H \tag{12}$$

In this case, we obtain existence and uniqueness of bounded, self-adjoint, positive operators, P, $\hat{P} \in \mathcal{L}(H)$ such that the feedback gain operator B^*P is generally unbounded, but densely defined, i.e.

$$B^*P \in \mathcal{L}\Big(\mathcal{D}(A); U\Big)$$

and the compensator gain $\hat{P}C^* \in \mathcal{L}(H)$ (Adamian and Gibson, 1991; Gibson, 1979). If, in addition, the weight Q satisfies a "smoothing" assumption (Da Prato *et al.*, 1986),

$$\|Q^*QA\|_{\mathcal{L}(H)} \leq M \tag{13}$$

then it was shown in (Da Prato *et al.*, 1986) that the gain operator B^*P is in fact bounded from $H \to U$.

To give more physical significance to the estimator problem and the compensator design, we add noise terms to the input, $u(t)$, and output, $z(t)$, in the original system (1)–(2). Let $\theta(t)$, $\nu(t) \in L_2(0\infty; \Gamma)$ be the stationary zero mean, Gaussian white noise processes with covariances $\hat{Q}$ and $\hat{R}$ (resp.) that are added to the input and output of system (1)–(2). This choice of $\hat{Q}$ and $\hat{R}$, coupled with the choice of the compensator gain $\hat{P}C^*$ where $\hat{P}$ represents the constant error covariance, produces the minimum variance estimate $\hat{x}(t)$ of the full state $x(t)$ (Anderson and Moore, 1989).

Combining the state equation (5) and estimator (6) yields

$$\begin{bmatrix} \dot{x}(t) \\ \dot{\hat{x}}(t) \end{bmatrix} = \begin{bmatrix} A & -BF \\ KC & A - KC - BF \end{bmatrix} \begin{bmatrix} x(t) \\ \hat{x}(t) \end{bmatrix} = \mathcal{A} \begin{bmatrix} x(t) \\ \hat{x}(t) \end{bmatrix} \tag{14}$$

The separation principle reduces the above compensator design problem into two subproblems,

1. Solve the estimator problem via Kalman filter theory, i.e. find the optimal estimate $\hat{x}$,
2. Determine the feedback control law with form $u(t) = F\hat{x}(t)$ that will minimize the deterministic cost in (3), subject to the dynamics of (1), via LQR theory.

It has been shown by Lasiecka (1992) that under conditions (4), (11), (12), the *optimal* compensator (14) produces uniformly stabilizing feedback, i.e.,

$$\|e^{\mathcal{A}t}\|_{\mathcal{L}(H \times H)} \leq Ce^{-\omega t}, \quad \text{for some } \omega > 0$$

3. Variational Formulation

The variational formulation for system (1) is, for all $\phi \in \mathcal{D}(\mathcal{A}^{1/2}) \equiv H^2(\Omega) \cap H_0^1(\Omega)$,

$$(kw_{tt}, \phi)_\Omega - \gamma(\Delta w_{tt}, \phi)_\Omega + (\Delta^2 w, \phi)_\Omega = 0 \tag{15}$$

Applying Green's theorem and the boundary conditions, we get

$$(kw_{tt}, \phi)_\Omega + \gamma(\nabla w_{tt}, \nabla\phi)_\Omega + (\Delta w, \Delta\phi)_\Omega = \Big(u(t), \frac{\partial}{\partial\nu}\phi\Big)_\Gamma \tag{16}$$

At the level of approximation, we introduce a family of finite-dimensional subspaces

$$V_h \subset \mathcal{D}(\mathcal{A}^{1/2}) \equiv H^2(\Omega) \cap H_0^1(\Omega)$$

with orthogonal projection π_h: $H^2(\Omega) \cap H_0^1(\Omega)$ onto V_h. In order to ensure the convergence of the Riccati operators arising in the context of (11), (Hendrickson and Lasiecka, 1993), it is necessary to consider a regularization of the system by introducing certain *viscosity* boundary terms. This is to say that instead of (16) we consider the finite-dimensional, regularized variational formulation, with w^h, $\phi^h \in V_h$,

$$(kw_{tt}^h, \phi^h)_\Omega + \gamma(\nabla w_{tt}^h, \nabla\phi^h)_\Omega + (\Delta w^h, \Delta\phi^h)_\Omega + \epsilon_1(w_t^h, \phi^h)_\Omega \tag{17}$$

$$+\epsilon_1\gamma(\nabla w_t^h, \nabla\phi^h)_\Omega + \epsilon_2\Big(\frac{\partial}{\partial\nu}w_t^h, \frac{\partial}{\partial\nu}\phi^h\Big)_\Gamma = \Big(u^h(t), \frac{\partial}{\partial\nu}\phi^h\Big)_\Gamma$$

We apply a standard finite element algorithm to a special case when $\Omega \equiv [0,1]$, using the space of Hermite cubics defined on a uniform mesh of Ω. This procedure reduces the spatial and time differential equation into a time differential equation. We denote

$$V_h \subset \mathcal{D}(\mathcal{A}^{1/2}) \equiv \Big(v \in H^2(0,1) | v(0) = v(1) = 0\Big)$$

as the family of finite dimensional subspaces and choose basis functions $\phi_{ij}^h(x) \in V_h$, which are defined on a reference (local) element as

$$\hat{\phi}_{11}(\xi) = \frac{1}{4}(2 - 3\xi + \xi^3), \qquad \hat{\phi}_{21}(\xi) = \frac{1}{4}(2 + 3\xi - \xi^3)$$

$$\hat{\phi}_{12}(\xi) = \frac{1}{4}(1 - \xi - \xi^2 + \xi^3), \qquad \hat{\phi}_{22}(\xi) = \frac{1}{4}(-1 - \xi + \xi^2 + \xi^3)$$

with

$$\xi(x) = \frac{2x - (x_{i-1} + x_i)}{x_i - x_{i-1}}, \qquad -1 \le \xi \le 1$$

The displacement of the beam at an arbitrary time $t > 0$ is given as a linear combination of the basis functions that use the displacement and slope of the displacement at each node as data, i.e.,

$$w^h(x,t) = \sum_{i=1}^{N+1} \sum_{j=1}^{2} \alpha_{ij}(t)\phi_{ij}^h(x) \tag{18}$$

where $\alpha_{i1}(t) = w(x_i,t)$, and $\alpha_{i2}(t) = \dfrac{\mathrm{d}}{\mathrm{d}x}w(x_i,t)$ and $N+1$ is the number of equally spaced nodes. Applying (18) to the variational formulation (17), we get the following matrix representation of the FE system for the partial differential equation model of the Kirchoff plate,

$$M\ddot{\alpha}^{(h)} + K\dot{\alpha}^{(h)} + L\alpha^{(h)} = B^{(h)}u(t) \tag{19}$$

$$z(t) = H \begin{bmatrix} \alpha \\ \dot{\alpha} \end{bmatrix}$$

where M, K, L are $2N \times 2N$ matrices such that

$$M_{ij}^{(h)} = \int_0^1 \phi_{ij}\phi_{kl} + \gamma \frac{\mathrm{d}}{\mathrm{d}x}\phi_{ij}\frac{\mathrm{d}}{\mathrm{d}x}\phi_{kl}\,\mathrm{d}x \tag{20}$$

$$K_{ij}^{(h)} = \epsilon_1 M_{ij}^{(h)} + \epsilon_2 \frac{\mathrm{d}}{\mathrm{d}x}\phi_{ij}(0)\frac{\mathrm{d}}{\mathrm{d}x}\phi_{kl}(0)$$

$$L_{ij}^{(h)} = \int_0^1 \frac{\mathrm{d}^2}{\mathrm{d}x^2}\phi_{ij}\frac{\mathrm{d}^2}{\mathrm{d}x^2}\phi_{kl}\,\mathrm{d}x$$

and B is a $2N \times 1$ column vector with $B(1) = -1$, $B(j) = 0$, $j > 1$, and H is a $1 \times 4N$ row vector, with $H(1) = 1$, $H(j) = 0$, $j > 1$.

Further, since it is impractical to numerically calculate $M^{-1}K$, $M^{-1}L$, $M^{-1}B$, we perform a preliminary Cholesky transformation on M, $M = M_c M_c^T$, such that (19) becomes

$$\ddot{y} + K_m\dot{y} + L_m y = B_m u(t) \tag{21}$$

where $y = M_c^T \alpha$, $K_m = M_c^{-1} K M_c^{-T}$, $L_m = M_c^{-1} L M_c^{-T}$, $B_m = M_c^{-1} B$, or as a first order matrix differential equation

$$\begin{bmatrix} \dot{y} \\ \ddot{y} \end{bmatrix} = \begin{bmatrix} 0 & I \\ -L_m & -K_m \end{bmatrix} \begin{bmatrix} y \\ \dot{y} \end{bmatrix} + \begin{bmatrix} 0 \\ B_m \end{bmatrix} u(t)$$

$$= A_{eh} x_h + B_h u_h, \quad x_h = [y, \dot{y}]^T, \quad B_h = \begin{bmatrix} 0 \\ B_m \end{bmatrix} \tag{22}$$

This approximation scheme satisfies the usual consistency and stability properties that are required in the approximation theory, (Hendrickson and Lasiecka, 1993; Lasiecka, 1992).

4. Regularization Procedure and Results

As can be seen in the previous section, the implementation of the standard finite element method is straight-forward. But, when using numerical schemes in the context of computations of algebraic Riccati equations, certain conditions must be upheld by the method in order to ensure the *convergence* of the algorithm (Lasiecka, 1992). These conditions are as follows,

$$\|A_h^{-1}\pi_h - A^{-1}\|_H \to 0, \qquad x \in H \tag{23a}$$

$$\|(A^{-1} - A_h^{-1})\pi_h B u\|_H \to 0, \qquad u \in U \tag{23b}$$

$$\|A^{-1}(B_h - B)u\|_H \to 0, \qquad u \in U \tag{23c}$$

$$\|(A_h^{-1} - A^{-1})B_h u\|_H \to 0, \qquad u \in U \tag{23d}$$

(A_h, B_h), $(A_h{}^*, \pi_h C^*)$ are uniformly stabilizable with respect to h (24)

(A_h, Q_h), $(A_h{}^*, \hat{Q}_h)$ are uniformly detectable with respect to h (25)

as well as the discrete trace regularity condition

$$\int_0^T \|B_h^* e^{A_h{}^* t} \pi_h x\|_U^2 \le C_T \|x\|_H^2 \tag{26a}$$

$$\|Q_h^* Q_h A_h x_h\|_H \le \|x\|_H \tag{26b}$$

where $Q_h = \pi_h Q$, $\hat{Q}_h = \pi_h \hat{Q}$. Recall that (A_h, B_h) are uniformly stabilizable iff there exists $F_h : V_h \to U$, and constants $\omega_B > 0$, $M > 0$ such that

$$\|e^{(A_h + B_h F_h)t}\|_{\mathcal{L}(H)} \le C e^{-\omega_B t}, \quad \text{uniform in } h$$

and that at the finite dimensional level, uniform detectability of (A_h, C_h) holds iff the discrete pair $(A_h{}^*, C_h^*)$ is uniformly stablizable. Under conditions (23)–(26),

the desired convergence properties of the solutions P_h, $\hat{P}_h \in \mathcal{L}(H)$ to the discrete algebraic Riccati equations,

$$A_h^T P_h + P_h A_h - P_h B_h R^{-1} B_h^* P_h + Q_h = 0 \tag{27}$$

$$A_h \hat{P}_h + \hat{P}_h A_h^T - \hat{P}_h C_h^* \hat{R}^{-1} C_h \hat{P}_h + \hat{Q}_h = 0 \tag{28}$$

as well as the gains $B_h^* P_h$, $\hat{P}_h \pi_h C^*$ are proved by Lasiecka (1992). Using the solutions to (27)–(28), we choose our finite-dimensional feedback and compensator gains to have the forms,

$$F_h \equiv -B_h^* P_h \tag{29}$$

$$K_h \equiv \hat{P}_h \pi_h C^* \tag{30}$$

We specify the operators R_h, $\hat{R}_h$, Q_h, $\hat{Q}_h$ to be

$$R_h = \hat{R}_h = \alpha \Pi_h, \quad Q_h x^h = \hat{Q}_h x^h = Q_h \begin{pmatrix} w^h \\ w_t^h \end{pmatrix} = \begin{pmatrix} 0 \\ w^h \end{pmatrix} \tag{31}$$

It should be noted that the standard FEM, when applied to the original problem (1) with $\epsilon_1 = \epsilon_2 = 0$, fails to satisfy the criteria in (23)–(26), (Banks *et al.*, 1991; Hendrickson and Lasiecka, 1993). For this reason, to prevent the loss of uniformity at the level of approximation, (Hendrickson and Lasiecka, 1993) proposed a regularization and approximation scheme which assures that conditions (23)–(26) are satisfied by the approximation. Consequently, it was proved in (Hendrickson and Lasiecka, 1993) that the Riccati operators and corresponding gains are convergent for the regularization scheme. The ϵ_1 regularization term serves to guarantee that the uniform stabilizability conditions are satisfied, while the ϵ_2 regularization term acts to provide that the uniform trace regularity condition (26a) is maintained by the approximation scheme. This algorithm is outlined below.

Step 1. Initially, the regularization of the entire system (full state $x(t)$ and dynamic estimator $\hat{x}(t)$) is performed such that the feedback gain F and compensator gain K depend upon the regularized dynamics A_ϵ, and are denoted F_ϵ (resp. K_ϵ). Hence, the system becomes

$$\frac{\mathrm{d}}{\mathrm{d}t} \begin{pmatrix} x \\ \hat{x} \end{pmatrix} = \mathcal{A}_\epsilon \begin{pmatrix} x \\ \hat{x} \end{pmatrix} = \begin{pmatrix} A_\epsilon & BF_\epsilon \\ K_\epsilon C & A_\epsilon + BF_\epsilon - K_\epsilon C \end{pmatrix} \begin{pmatrix} x \\ \hat{x} \end{pmatrix} \tag{32}$$

Step 2. Performing step 1 avoids the failure, at the implementation level, of the chosen approximation scheme to maintain uniformly the asymptotic stability properties of the continuous system. But these schemes, now applied to (32), inherently preserve the asymptotic stability properties, uniformly in h and guarantee the convergence of the Riccati operators, (Hendrickson, 1994). The next step in the procedure follows from the finite dimensional approximation to the regularized estimator with $\epsilon = (\epsilon_1, \epsilon_2)$,

$$\frac{\mathrm{d}}{\mathrm{d}t} \hat{x}_h(t) = (A_{\epsilon h} \pi_h + B_h F_{\epsilon h} \pi_h) \hat{x}_h(t) + K_{\epsilon h} C \Big(x(t) - \hat{x}_h(t) \Big) \tag{33}$$

and the regularized, finite dimensional control law

$$u_{\epsilon h}(t) = F_{\epsilon h}\pi_h \hat{x}_h(t) \tag{34}$$

The new system becomes

$$\frac{\mathrm{d}}{\mathrm{d}t}\begin{pmatrix} x \\ \hat{x}_h \end{pmatrix} = \bar{\mathcal{A}}_{h,\epsilon}\begin{pmatrix} x \\ \hat{x}_h \end{pmatrix}$$

$$= \begin{pmatrix} A_\epsilon & BF_{\epsilon h}\pi_h \\ K_{\epsilon h}C & A_{\epsilon h}\pi_h + B_h F_{\epsilon h}\pi_h - K_{\epsilon h}C \end{pmatrix}\begin{pmatrix} x \\ \hat{x}_h \end{pmatrix} \tag{35}$$

Notice that the discretization procedure in step 2 did not affect the (1,1) term in (35). This term represents the continuous dynamics of the regularized system. We do not wish to finite-dimensionalize the original dynamics, and we shall see in the last step that we recover the original, continuous, full state dynamics. The process fits in with the design goal of developing a finite dimensional compensator that produces near optimal performance when applied to the original, continuous dynamics.

Step 3. Since we desire the finite dimensional compensator to act upon the original, continuous dynamics, while obeying the control law (34), we have

$$\frac{\mathrm{d}}{\mathrm{d}t}x(t) = Ax(t) + BF_{\epsilon h}\pi_h \hat{x}_h(t) \tag{36}$$

Considering this, we arrive at the ultimate approximation

$$\frac{\mathrm{d}}{\mathrm{d}t}\begin{pmatrix} x \\ \hat{x}_h \end{pmatrix} = \mathcal{A}_{h,\epsilon}\begin{pmatrix} x \\ \hat{x}_h \end{pmatrix}$$

$$= \begin{pmatrix} A & BF_{\epsilon h}\pi_h \\ K_{\epsilon h}C & A_{\epsilon h}\pi_h + B_h F_{\epsilon h}\pi_h - K_{\epsilon h}C \end{pmatrix}\begin{pmatrix} x \\ \hat{x}_h \end{pmatrix} \tag{37}$$

The main result is summarized in the following theorem.

Theorem 1. *For the continuous problem (1)-(2), assume that both regularity conditions (4), (13) hold, as well as the stabilizability/detectability conditions (11)-(12). Assume that conditions (23)-(26) hold for the standard finite element approximation to (1)-(2). Then, if the feedback gain is given as in (7), (resp. (29)), and the estimator gain has form (8), (resp. (30))*

Then, for $\epsilon_1 > 0$ fixed and for all $\bar{x} = (x, w) \in \mathcal{H} \equiv H \times H$, there exists $\epsilon_0 > 0$ such that for all $\epsilon < \epsilon_0$ there is some $h_0(\epsilon)$ such that for all $h < h_0$,

$$\|e^{\mathcal{A}_{h,\epsilon}t}\bar{x}\|_{L_2(0\infty;\mathcal{H})} \leq C\|\bar{x}\|_{\mathcal{H}}, \quad t \in [0,T] \tag{38}$$

(Convergence of controls)

$$\lim_{\epsilon_2 \to 0}\lim_{h \to 0}\|u_{h,\epsilon} - u\|_{L_2(0\infty;U)} = 0 \tag{39}$$

(Convergence of gains)

$$\lim_{\epsilon_2 \to 0} \lim_{h \to 0} \|F_{\epsilon h}\bar{x} - F\bar{x}\|_U = 0 \tag{40}$$

(Convergence of Performance Index)

$$\lim_{\epsilon_2 \to 0} \lim_{h \to 0} J\Big(u_{h,\epsilon}, x(u_{h,\epsilon})\Big) - J\Big(u, x(u)\Big) = 0 \tag{41}$$

(Uniform stability)

There exists $\omega_0 > 0$ *such that for all* $\bar{x} = (x, 0)$,

$$\|e^{\mathcal{A}_{h,\epsilon}t}\bar{x}\|_{\mathcal{H}} \leq Ce^{-\omega_0 t}\|\bar{x}\ |_{\mathcal{H}} \tag{42}$$

Remarks:

1. The result in Theorem 1 requires the original system to be weakly damped (Russell, 1975), which is satisfied by fixing $\epsilon_1 > 0$. However, letting $\epsilon_1 \to 0$ recover the convergence properties of the performance index but the *uniform* stability of $e^{\mathcal{A}_{\epsilon_1,\epsilon_2,h}t}$ would be lost.
2. Lasiecka (1992) proved the convergence of the compensators $e^{\mathcal{A}_{h,0}t}$ $(\epsilon = 0)$ under *additional* conditions that

$$\int_0^T \|B_h{}^* e^{A_h^* t}x\|_U^2 \leq C\|x\|_H^2 \quad \text{uniformly } in \quad h > 0 \tag{i}$$

$$(A_h, B_h) \quad \text{are uniformly stabilizable} \tag{ii}$$

   Since the above assumptions may fail for certain convergent approximations such as FEM, the main point for introducing the regularization was to avoid requirement (i) and (ii).
3. Under the minimal approximation hypotheses for stability and consistency, the main result of Theorem 1 provides an algorithm for the construction of a finite dimensional control $u_{h,\epsilon}$ which, when inserted into the original system, gives a near optimal performance of the system. The resulting compensator system retains the uniform stability properties (see (42)), provided that the initial condition for the estimator equation, i.e. w_0, is sufficiently regular. Typically $w_0 = 0$, so that this regularity requirement is satisfied automatically. But, the need to assume higher regularity for initial condition w_0 results from an interesting new feature of the problem which is the lack of a uniform C_0-semigroup estimate for the operator $e^{\mathcal{A}_{h,\epsilon}t}$. In fact, $e^{\mathcal{A}_{h,\epsilon}t}$ is a one time integrated semigroup while $\|e^{\mathcal{A}_{h,\epsilon}t}\|_{\mathcal{L}(\mathcal{H})}$ is of order $(\frac{1}{\sqrt{\epsilon_2}})$.

5. Effect of Regularization on the Open-Loop Problem

The purpose of the regularization process is to guarantee that the uniform stabilizability and uniform trace assumptions (Hendrickson and Lasiecka, 1993; Lasiecka, 1992) are satisfied by such desirable schemes as finite elements (Banks *et al.*, 1991;

for an example of a weakly damped wave equation failing to satisfy these conditions). Without any damping, the spectrum of the open-loop system lies on the imaginary axis. The ϵ_1 term, in effect, shifts the spectrum into the open left-half plane along a vertical line, as seen in Fig. 1.

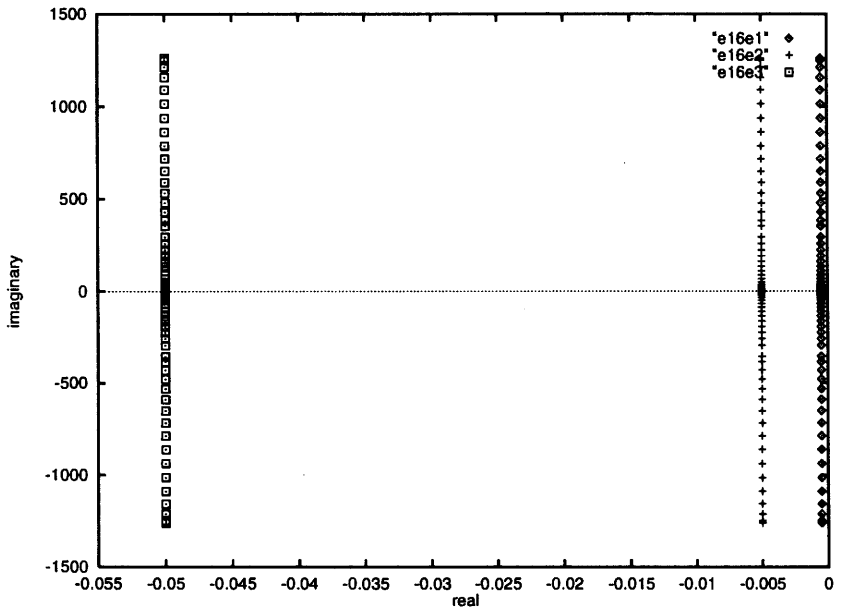

Fig. 1. Open-loop spectrum with $\epsilon_1 = .001(\diamond)$, $= .01(+)$, $= .1(\square)$, $\epsilon_2 = 0$.

Remark 2. If the interior regularization term is $\epsilon_1 w_t$ rather than $\epsilon_1(w_t - \gamma \Delta w_t)$, then we observe in Fig. 2 that the lower frequencies have larger negative real parts, i.e. are more highly damped, than the higher frequencies. More importantly, we see that as the number of elements increases, then higher frequncies asymptotically approach the imaginary axis. Again, this effect is due to the fact that the regularization term can be written abstractly as a compact operator, and uniform stabilization cannot be achieved by a compact operator (Gibson, 1980; Russell, 1975; Triggiani, 1975; 1989).

In Figs. 3 and 4 we see the effect of the ϵ_2-term. We observe that for $.0001 \leq \epsilon_2 \leq .0005$ the high eigenfrequencies are more highly damped than the lower frequencies. But for $.001 \leq \epsilon_2$, the higher eigenfrequencies appear to tend towards the imaginary axis, although never reaching the imaginary axis. For $\epsilon_2 = .1$ we observe that the entire spectrum begins to shift towards the imaginary axis. This observation confirms that the decay rates are not proportional to the damping coefficients. Due to this phenomena, the choice of the magnitude of the boundary regularization term must be carefully selected to avoid an undesirable shift of the open-loop spectrum.

6. Linear Quadratic Regulator

The stabilization of the beam with a non-zero initial state can be brought to rest by constructing a control using state feedback based on the solution to an algebraic

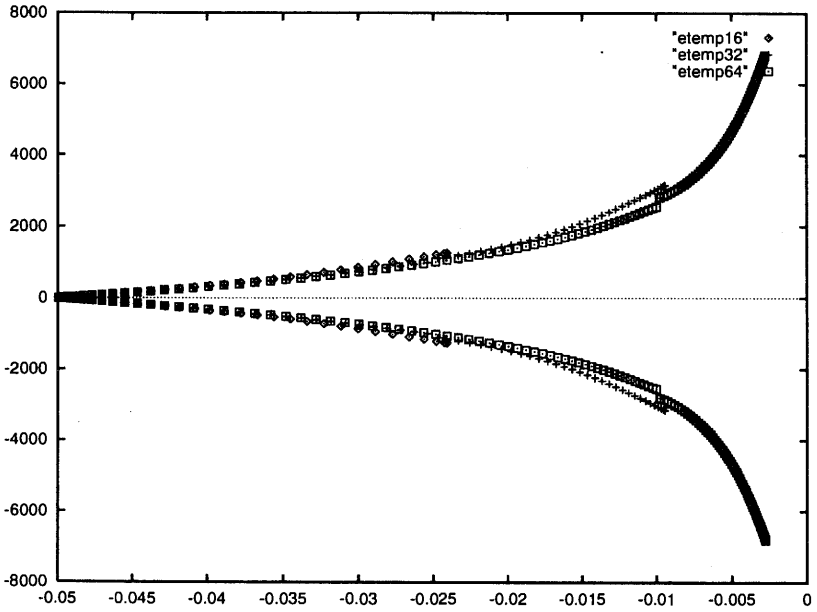

Fig. 2. Open-loop spectrum with $\epsilon_1 = .1$, $N = 16(\diamond)$, $N = 32(+)$, $N = 64(\square)$, $\epsilon_2 = 0$

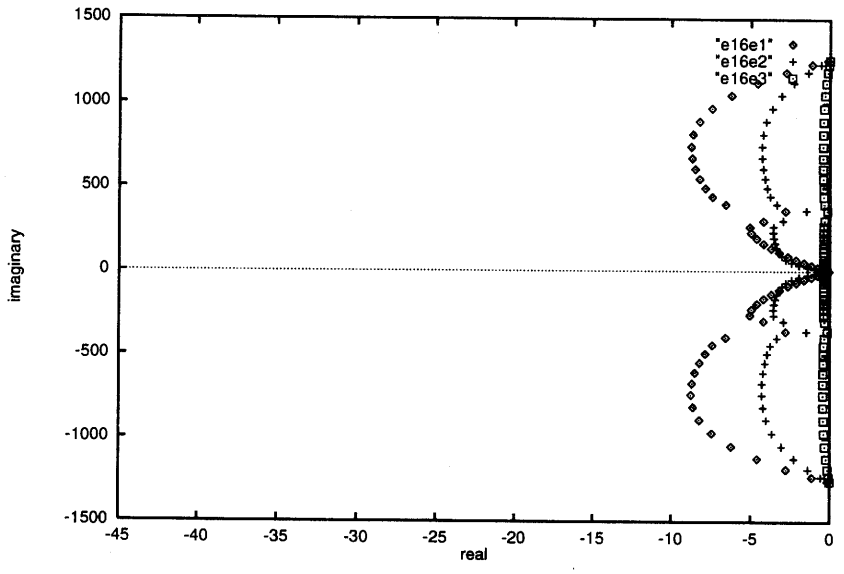

Fig. 3. Open-loop spectrum with $\epsilon_1 = 0$, $\epsilon_2 = .005(\diamond)$, $.01(+)$, $.1(\square)$.

Riccati equation. The cost functional in (3) is reduced, via the approximation by finite elements, to the familiar finite dimensional functional,

$$J\Big(u_h, x_h(u_h)\Big) = \int_0^\infty \Big(x_h^T(t)Q_h x_h(t) + u_h^T(t)R_h u_h(t)\Big)\ \mathrm{d}t \tag{45}$$

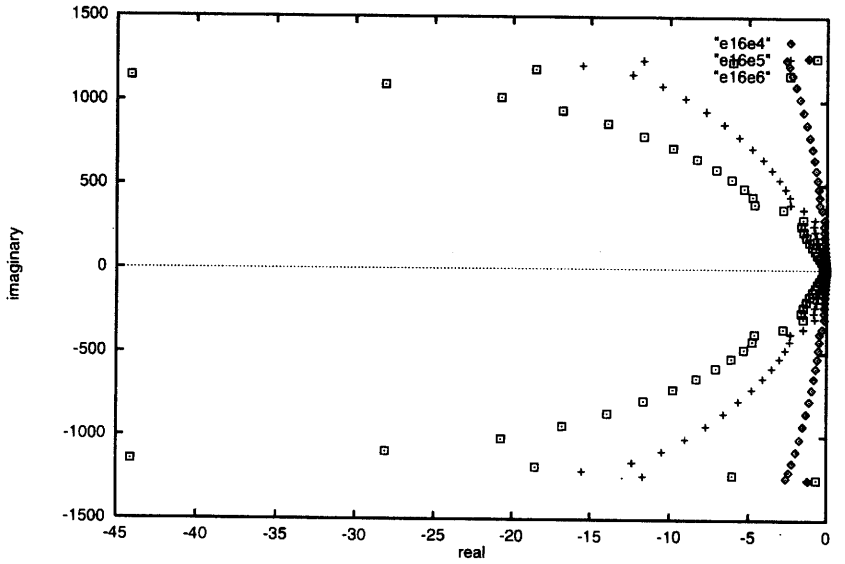

Fig. 4. Open-loop spectrum with $\epsilon_1 = 0$, $\epsilon_2 = .0001(\diamond)$, $.0005(+)$, $.001(\square)$.

where $x_h(t)$ is the state vector consisting of displacements, slopes, and their velocities, and $u_h(t)$ is the control vector. After the Cholesky decomposition performed earlier on the state $x_h(t)$, the matrix Q_h in (31) becomes

$$Q_h = \begin{bmatrix} I & 0 \\ 0 & 0 \end{bmatrix} \tag{46}$$

This matrix Q_h represents the transformed matrix representation with respect to the H-inner product of the Q term satisfying a smoothing assumption (26b).

The following graphs plot the optimal control, $u_h^0(t) = -B_h^* P_h x_h(t)$, against time, for $N = 4, 8, 16$ and P_h is the solution to the associated matrix algebraic Riccati equation. The initial state is taken to be the first mode, $\sin \pi x$ (Figs. 5 and 6).

Remark 3. We can intepret the magnitude and sign of the control $u(t)$ as the magnitude of the torque applied at the $x = 0$ end and the sign as corresponding to the clockwise or counterclockwise direction to which the torque is applied.

We observe that the optimal control $u^0(t) \to 0$ as $t \to \infty$. The amplitude of the regularized control is slightly less than that of the unregularized control, due to the damping introduced by the regularization. Next, we examine the stabilization of the midpoint of the beam when the beam has an initial displacement, $\sin \pi x$. The interior regularization term (viscous damping) causes a slightly faster decay rate, as expected.

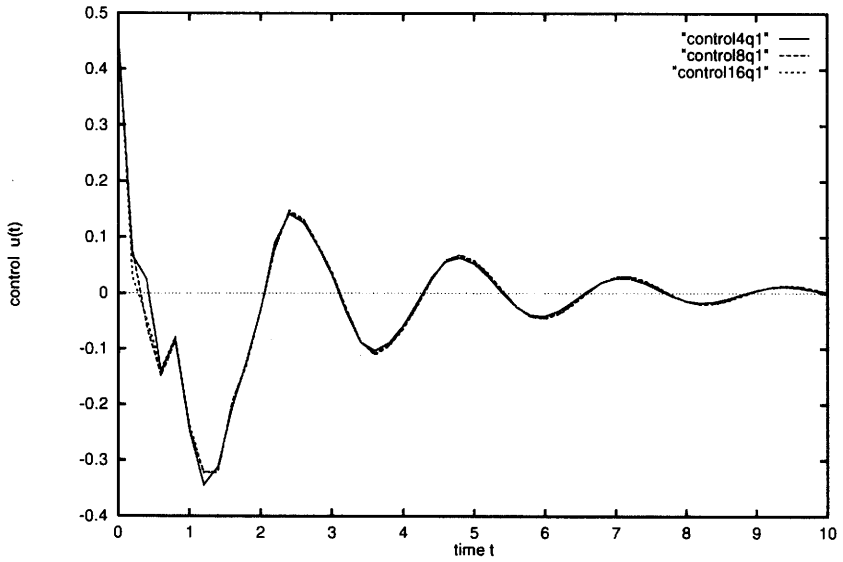

Fig. 5. $u(t)$ vs. t, for $N = 4, 8, 16$.

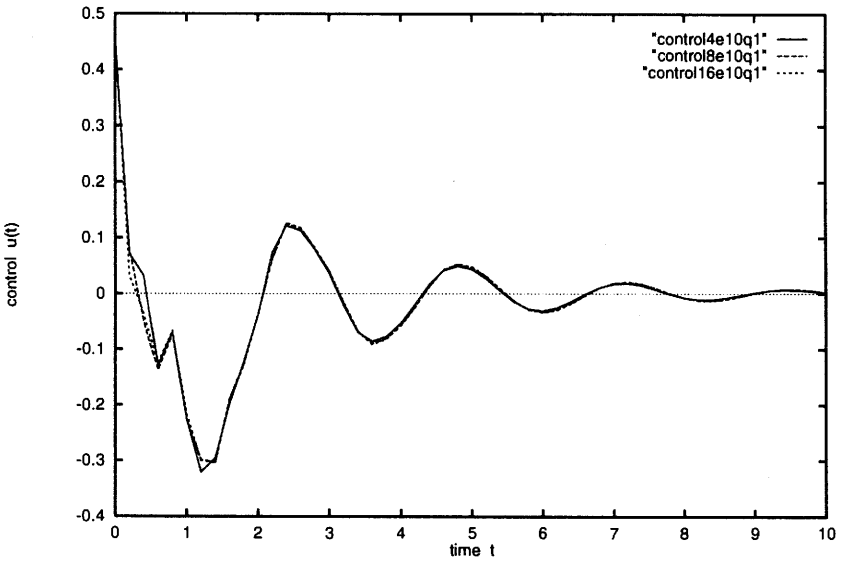

Fig. 6. $u(t)$ vs. t, for $N = 4, 8, 16$, $\epsilon_1 = .1$, $\epsilon_2 = .00001$.

The effect of regularization coupled with the design parameter Q_h is quite apparent on the spectrum of the closed-loop poles. In Fig. 8, we compare $\sigma(A - BB^*P)$ vs. $\sigma(A_\epsilon - BB^*P_\epsilon)$ for three cases: (i) $\epsilon_1 = .001\epsilon_2 = 0.0$ ($\diamond$), (ii) $\epsilon_1 = \epsilon_2 = .01$ (+), and (iii) $\epsilon_1 = .1$, $\epsilon_2 = .00001$ ($\square$). We have taken Q_h to be as in equation (44).

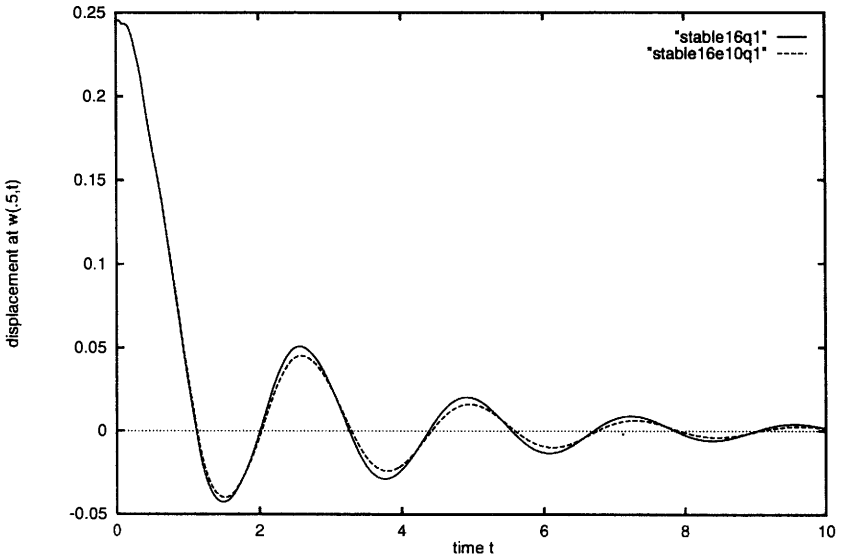

Fig. 7. Stabilization of midpoint for $N = 16$: $\epsilon_1 = \epsilon_2 = 0$, $\epsilon_1 = .1$ $\epsilon_2 = .00001$.

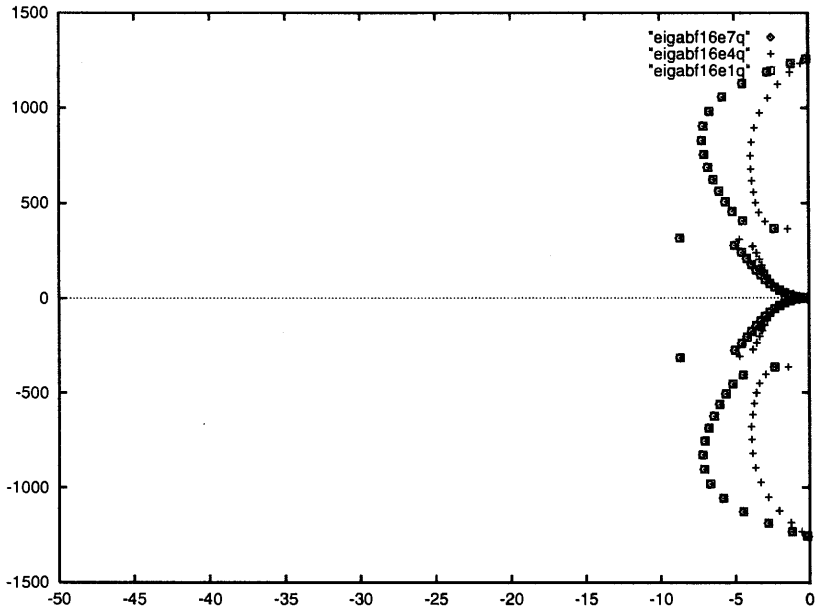

Fig. 8. Closed-loop poles for N=16: $\epsilon_1 = \epsilon_2 = 0$, $\epsilon_1 = \epsilon_2 = .01$, $\epsilon_1 = .1\epsilon_2 = .00001$.

Notice that the structures of the regularized closed-loop poles are very similar to the open-loop poles with boundary regularization. This seems to show, in this example, that the feedback control $u^0(t)$ has a similar effect to a viscous damping term with large magnitude on the boundary. Also, the choice of the state penalty

term Q determines the character of the closed-loop spectrum, while the regularization parameters act to produce spectrums of only slight variations from the original, unregularized system.

Remark 4. If we recall from the abstract formulation of the Kirchoff plate in (1) that

$$u^0(t) = -B^*Px(t) = -\frac{\partial}{\partial \nu}P(w, w_t)$$

we recognize the similar construction between the form of the Riccati-based, feedback control and the boundary regularization term, $\epsilon_2 \frac{\partial}{\partial \nu} w_t(0,t)$.

Also, since Q_h satisfies the "smoothing" assumption (26b) which yields a bounded gain operator $B_h^* P_h$, the effect of the control on the higher frequencies is less.

If the cost functional penalizes the energy of the state instead of the H^1-norm of the displacement (i.e. $Q = I$ in the performance index (3)), then the Q_h matrix becomes, after the decomposition and variable change,

$$Q = \begin{bmatrix} L_m & 0 \\ 0 & I \end{bmatrix} \tag{47}$$

This choice of Q_h does not satisfy the smoothing hypothesis (26b), hence the conclusions of Theorem 1 do not apply for this Q_h. But it is interesting to note how this Q_h affects the associated LQR problem, in particular the change of the distribution of $\sigma(A_h - B_h B_h^* P_h)$. Here, the feedback control has a stronger effect on the high frequency modes than with the previous choice of Q_h. The observation is due to the result that the gain B^*P is now an unbounded, but densely-defined operator on H. Figure 9 illustrates the loss of uniform stability in the closed-loop spectrum of the unregularized system. We see that as N increases, the eigenvalues move to the right towards the imaginary axis. The magnitudes of the $Re\sigma(A_h - B_h B_h^* P_h)$ are significantly less than those resulting from the Q_h in (44). This confirms that regularization is necessary to achieve *numerical* stability of the margin of uniform decay.

When regularization is applied to the system, the resulting closed-loop system maintains the uniform stability, asserted in the theory. Figure 10 reflects this outcome.

We next see the plot of the optimal control for the Q in (45). We observe that the amplitudes of oscillation of the control decrease very slowly, unless a sufficient amount of interior damping is added.

The settling time for the midpoint of the beam is several seconds, even with interior damping present (Fig. 12). Several factors contribute to the long settling time, including the choices of Q and R, as well as the physical parameters describing the plate flexibility.

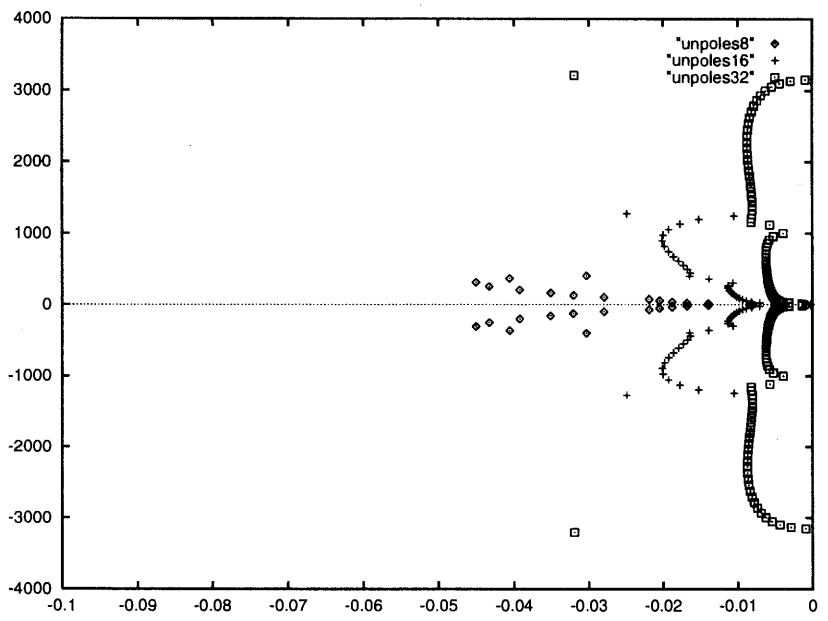

Fig. 9. Closed-loop poles for $N = 8, 16, 32$ with $\epsilon_1 = \epsilon_2 = 0$: $N = 8$ ($\diamond$), $N = 16+$, $N = 32$ ($\square$).

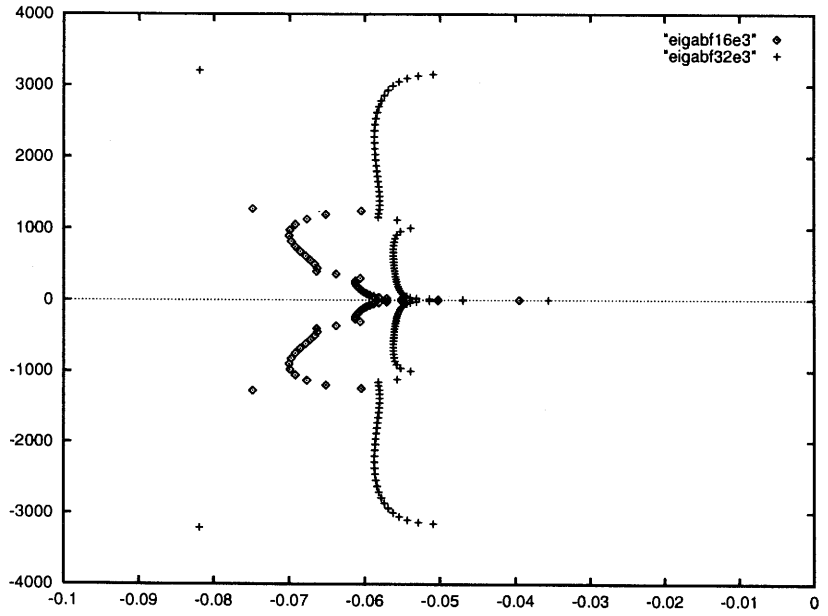

Fig. 10. Closed-loop poles for $N = 16, 32$ with $\epsilon_1 = .1$ $\epsilon_2 = 0$: $N = 16$ ($\diamond$), $N = 32(+)$.

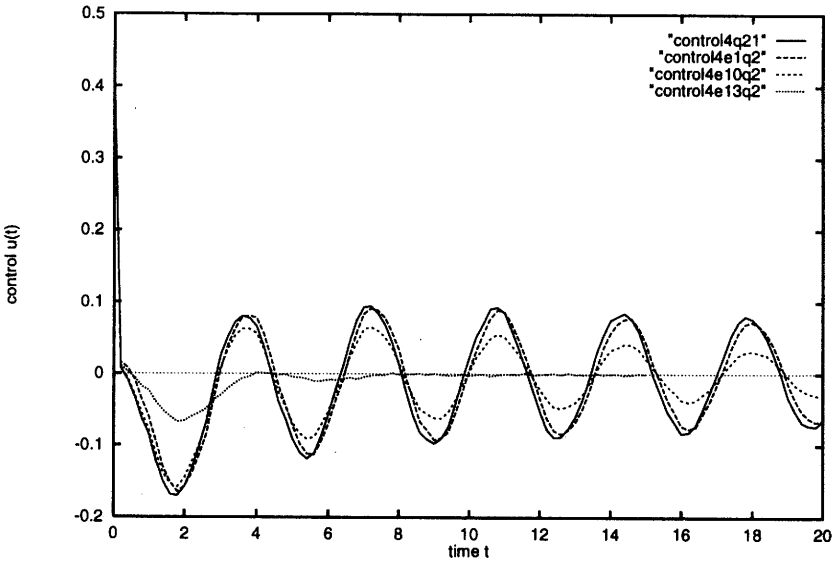

Fig. 11. $u(t)$ vs. t : $\epsilon_1 = \epsilon_2 = 0$, $\epsilon_1 = \epsilon_2 = .01$, $\epsilon_1 = .1$ $\epsilon_2 = .00001$, $\epsilon_1 = 1$ $\epsilon_2 = 0$.

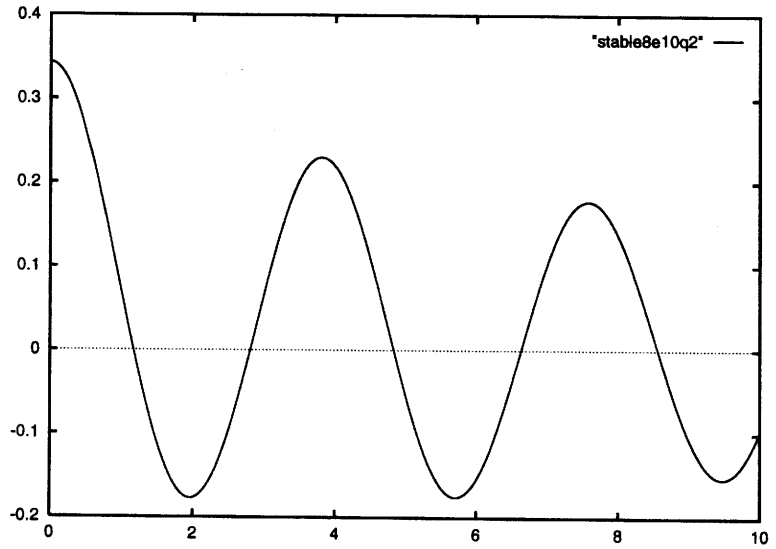

Fig. 12. Stabilization of the midpoint for $N = 8$: $\epsilon_1 = .1$, $\epsilon_2 = .00001$.

The settling speed of the beam can be adjusted by tuning the control weight R. We find that the decay of the transients is greatest for larger R. Figure 13 examines the settling time of the midpoint of the beam with $R = .1,\ 1,\ 10,\ 100$.

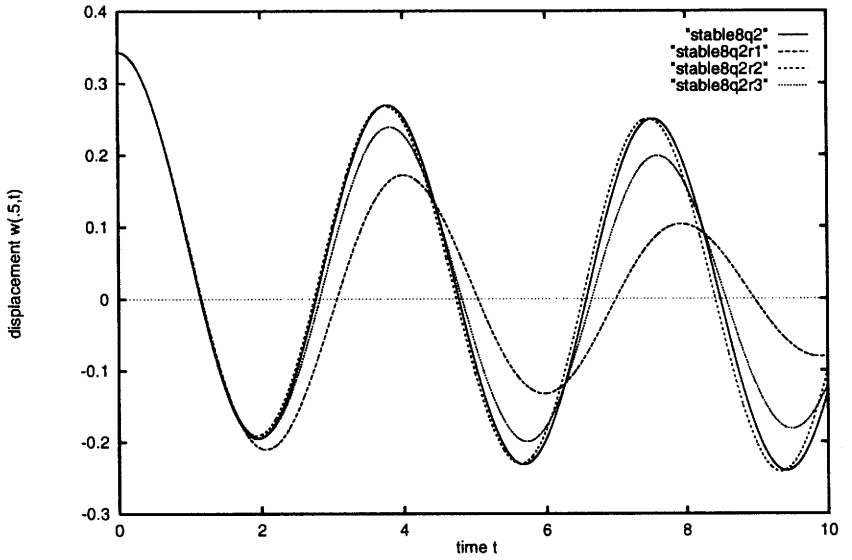

Fig. 13. Stabilization of the midpoint for $N = 8$: $R = .1, 1, 10, 100$.

The following table provides convergence results for the feedback gains with Q as in (45). In the norm evaluation, we take the projection of the first mode, $\sin \pi x$, and compute the $L_2(\Gamma)$ norm.

Table 1. Table of feedback gains.

N	ϵ_1	ϵ_2	$\|B^* P \pi_h x\|_{L_2(\Gamma)}$	$\|N_i - N_{i-1}\|$
4	0.0	0.0	.4103374247	
8	0.0	0.0	.4060941806	4.24324E-3
16	0.0	0.0	.4050818062	1.01237E-3
32	0.0	0.0	.4048344324	2.47374E-4
4	0.01	0.01	.410537790	
8	0.01	0.01	.406297160	4.24063E-3
16	0.01	0.01	.405285026	1.01214E-3
4	0.01	0.0	.410542991	
8	0.01	0.0	.406302556	4.24143E-3
16	0.01	0.0	.405290440	1.10121E-3
4	0.1	0.0001	.412352966	
8	0.1	0.0001	.408137198	4.21576E-3
16	0.1	0.0001	.407127355	1.00984E-3
4	0.1	0.00001	.412353132	
8	0.1	0.00001	.408137366	4.21576E-3
16	0.1	0.00001	.407127523	1.00984E-3

If we chose Q_h as in (44), we expect the "smoothing" effect by this term to provide better convergence results for the gains when compared with the Q_h from (45).

Also we see that the behaviour of the gains depends more on the choice of Q than on the regularization parameters. Although, the regularized gains give slightly better convergence rates than the unregularized gains as long as the boundary regularization term is chosen to be small with respect to the interior regularization term. The rates of convergence of the feedback gains for Q in (45) are significantly less that for (44), as we see in Tab. 5. Here, we take a projection of a function in H, but not in a dense subspace of H. The function used is

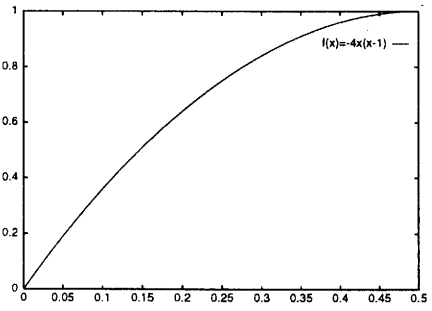

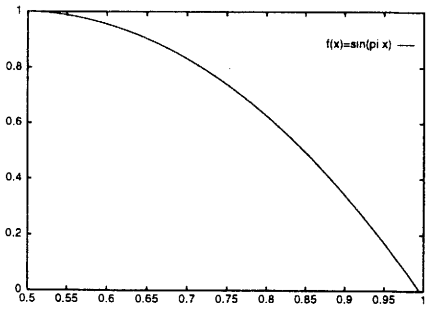

$$f(x) = -4x(x-1),\ 0 \le x \le .5, \qquad f(x) = \sin(\pi x),\quad .5 \le x \le 1$$

where the third derivative is not an $L_2(0,1)$ function.

Table 2. Table of feedback gains.

N	ϵ_1	ϵ_2	$\|B^*P\pi_h x\|_{L_2(\Gamma)}$	$\|N_i - N_{i-1}\|$
4	0.0	0.0	1.060237698	
8	0.0	0.0	1.061722961	1.48526E-3
16	0.0	0.0	1.062162030	4.39069E-4
32	0.0	0.0	1.062329752	1.67722E-4
4	0.01	0.01	1.020574611	
8	0.01	0.01	1.022192353	1.61774E-3
16	0.01	0.01	1.022656556	4.64203E-4
4	0.01	0.0	1.058490539	
8	0.01	0.0	1.059972368	1.48182E-3
16	0.01	0.0	1.060411031	4.38663E-4
4	0.1	0.0001	1.042623230	
8	0.1	0.0001	1.044074828	1.45160E-3
16	0.1	0.0001	1.044509881	4.35053E-4
4	0.1	0.00001	1.042974428	
8	0.1	0.00001	1.044425883	1.45145E-3
16	0.1	0.00001	1.044860920	4.35037E-4

If we change Q_h to be as in (45) and use the function given above, then the strong convergence results for the feedback gains are not provided for in theory and the following results support this conclusion. Notice that as N increases, we see the absolute errors of the feedback gains remain constant.

Table 3. Table of feedback gains

N	ϵ_1	ϵ_2	$\|B^*P\pi_h x\|_{L_2(\Gamma)}$	$\|N_i - N_{i-1}\|$
4	0.0	0.0	2.6619197344	
8	0.0	0.0	2.9859345307	3.24014E-1
16	0.0	0.0	3.3089636957	3.23029E-1
4	0.1	0.00001	2.6167926367	
8	0.1	0.00001	2.9406881592	3.23895E-1
16	0.1	0.00001	3.2637029992	3.23014E-1

7. Observer Design

Recall the form of the dynamic observer

$$\dot{\hat{x}}(t) = A\hat{x}(t) + Bu(t) + K\Big(z(t) - C\hat{x}(t)\Big) \tag{48}$$

where A, B are as in (20) and C is a $1 \times 4N$ row vector with $C(1) = 1.0$, $C(i) = 0.0$, $i > 1$. Combining the estimator and the state equation yields the matrix equation

$$\begin{bmatrix} \dot{x}(t) \\ \dot{\hat{x}}(t) \end{bmatrix} = \begin{bmatrix} A & -BF \\ KC & A - KC - BF \end{bmatrix} \begin{bmatrix} x(t) \\ \hat{x}(t) \end{bmatrix} \tag{49}$$

The compensator is based on the estimated state, obeying the control law

$$u(t) = F\hat{x}(t) \tag{50}$$

and F will be based on the solution to the appropriate algebraic Riccati equation. We can rewrite the above system via a similarity transformation as

$$\begin{bmatrix} \dot{x}(t) - \dot{\hat{x}}(t) \\ \dot{\hat{x}}(t) \end{bmatrix} = \begin{bmatrix} A - KC & 0 \\ KC & A - BF \end{bmatrix} \begin{bmatrix} x(t) - \hat{x}(t) \\ \hat{x}(t) \end{bmatrix} \tag{51}$$

We have already examined the infinite time horizon LQR problem for the system, hence we will refer to the previous section for results concerning the feedback gains (convergence) of the form

$$F = -R^{-1}B^*P \tag{52}$$

where $P = P^* \geq 0$ solves the matrix algebraic Riccati equation

$$A^TP + PA - PBR^{-1}B^*P + Q = 0 \tag{53}$$

Remark 5. Recall that the infinite-time regulator problem is to find $u(t) \in L_2(0\infty;\Gamma)$ that minimizes (3) when the system has zero noise processes and the full state as output. The minimum variance estimate of $x(t)$ satisfies (37), given the output $z(t)$. The optimal compensator gain K satisfies the form

$$K = \hat{P}C^*\hat{R}^{-1} \tag{54}$$

where $\hat{P} = \hat{P}^* \geq 0$ solves the matrix algebraic Riccati equation

$$A\hat{P} + \hat{P}A^T - \hat{P}C^*\hat{R}^{-1}C\hat{P} + \hat{Q} = 0 \tag{55}$$

and represents the constant error covariance. Hence, this procedure determines K such that the matrix $A - KC$ is exponentially stable and produces the minimum variance estimate of the full state $x(t)$ (Anderson and Moore, 1989).

In our simulation we consider $\hat{Q}$, $\hat{R}$ as parameters and examine how these terms affect the gain convergence as well as the error decay rates.

Remark 6. Another method of determining K such that $A - KC$ is exponentially stable is via pole placement, which is possible under the stabilizability and detectability conditions. But this method does not necessarily produce the minimum variance estimate of the full state $x(t)$. This method may be desired if certain error decay rates are required.

The following table provides convergence results for the estimator gains, K. In the norm evaluation, we take the L_2-projection of $\sin \pi x$ and compute the $L_2(\Gamma)$-norm of $K^* = C^T\hat{P}$. For these results, we take

$$\hat{Q} = \alpha \begin{bmatrix} I & 0 \\ 0 & I \end{bmatrix}, \qquad \hat{R} = 1 \tag{56}$$

Table 4. Table of estimator gains.

N	α	ϵ_1	ϵ_2	$\|C^*\hat{P}\pi_h x\|_{L_2\Gamma}$	$\|N_i - N_{i-1}\|$	max (real(λ_i))
4	1	0.01	0.00001	.9007208167		-3.24093E-1
8	1	0.01	0.00001	.9006375545	8.32626E-5	-3.34147E-1
16	1	0.01	0.00001	.9006375054	4.91239E-8	-3.84241E-1
4	100	0.01	0.00001	8.2125333541		-3.43417E-2
8	100	0.01	0.00001	8.2147065267	2.17317E-3	-4.94082E-2
16	100	0.01	0.00001	8.2149378433	2.31317E-4	-1.09796E-1
4	R=100	0.01	0.00001	.09816099636		-3.21135E-1
8	R=100	0.01	0.00001	.09814139841	1.95979E-5	-3.18319E-1
16	R=100	0.01	0.00001	.09814064244	7.55963E-7	-3.09710E-1

We see that the state weight, $\alpha = 100$, decreases the error decay rate. Changing the control weight $\hat{R}$ also affects the decay rate. (Xia and Manitius, 1993) observes an optimal value of $\hat{R}$ which causes the fastest decay rate for a fixed α. In the plot below, we observe that the initial error decays rapidly for the case when $N = 16$, $\hat{R} = 1$, $\alpha = 1$, $\epsilon_1 = .01$, and $\epsilon_2 = .00001$.

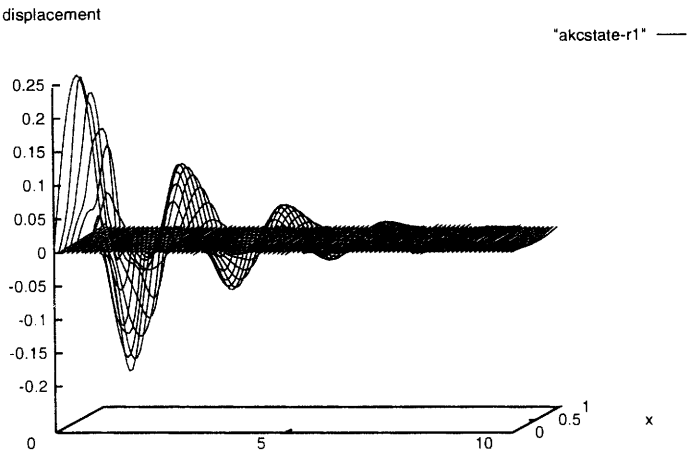

Fig. 14. Observer error decay in time, mode 1.

Also, by increasing $\hat{R}$ to 100, i.e, increasing the weight on the control, we see that the error settles rapidly and the frequency of oscillation, when compared to the $\hat{R} = 1$ case, decreases. We assertain that increasing α causes a reduction of the decay rate. We project that increasing $\hat{R}$ will move move the closed-loop spectrum towards the open-loop poles.

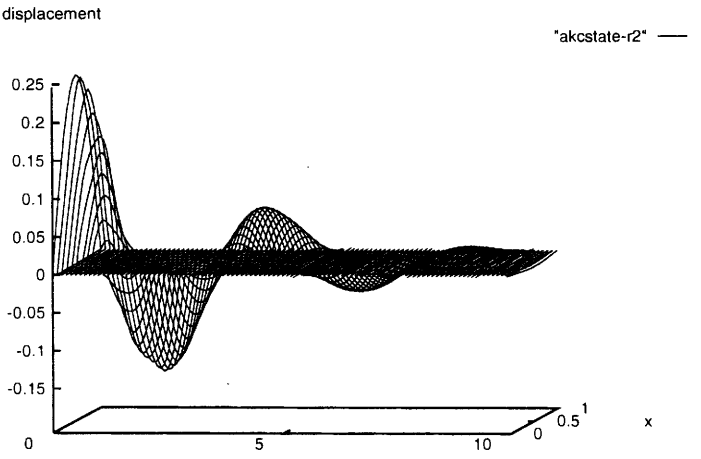

Fig. 15. Observer error decay in time, mode 1, $R = 100$.

If we choose $\hat{Q}$ to have the form

$$Q = \alpha \begin{bmatrix} 0 & 0 \\ I & I \end{bmatrix}, \qquad \hat{R} = 1 \tag{57}$$

then we get the following convergence results as seen in Tab. 5.

Table 5. Table of estimator gains.

N	α	ϵ_1	ϵ_2	$\|C^*\hat{P}\pi_h x\|_{L_2\Gamma}$	$\|N_i - N_{i-1}\|$	max (real(λ_i))
4	1.0	0.01	0.00001	.7556027158		-1.85624E-1
8	1.0	0.01	0.00001	.7587099045	3.10719E-3	-1.89531E-1
16	1.0	0.01	0.00001	.7596589864	9.49082E-4	-2.23588E-1
4	100	1.0	0.00001	7.6612995781		-6.51302E-1
8	100	1.0	0.00001	7.6610169515	2.82527E-4	-6.66233E-1
16	100	1.0	0.00001	7.6610672197	-5.02681E-5	-7.22639E-1
4	R=100	0.01	0.00001	.0774326618		-2.40037E-1
8	R=100	0.01	0.00001	.0774493157	1.66538E-5	-2.38333E-1
16	R=100	0.01	0.00001	.0774583759	9.06023E-6	-2.33571E-1

The damping needs to be increased when α is increased to maintain the stability of $\sigma(A - KC)$. We also notice that the decay rates vary as the forms of $\hat{Q}$ and $\hat{R}$ change. If we change the type of observation from a boundary observation to a point observation, we must add sufficient damping to the system to ensure that the stability assumptions are satisfied. Here, we take a point observation

$$y = Cx = c_0\delta(x - .5) \tag{58}$$

where $c_0 = 1$ and $x = .5$ is the midpoint of the beam. So, in the finite element formulation, C is a $1 \times 4N$ column row vector with $C(N) = 1$, $C(i) = 0$, $i \neq N$. We plot the observer error with $\hat{Q}$ as in (45) and $\epsilon_1 = 1.0$ and $\epsilon_2 = .00001$.

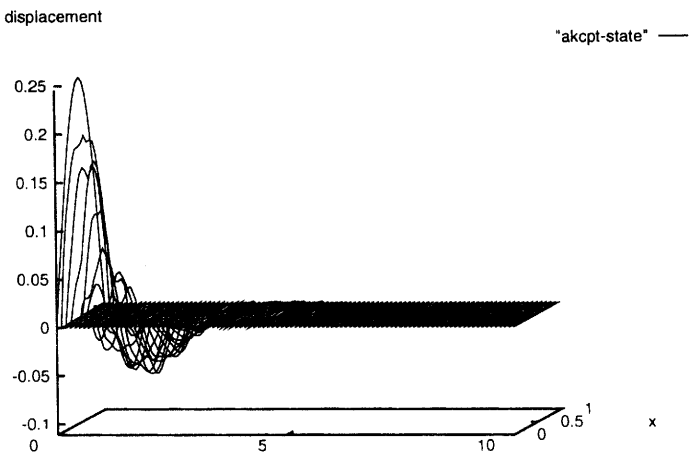

Fig. 16. Observer error decay in time, mode 1, midpoint observation.

Appendix

Description of Numerical Integration Technique

The numerical integration method following in the calculations in this research uses the LSODE.f routine from ODEPACK. We apply the time discretization scheme to the system in (22), rather than compute the discrete-time equivalent of the system in (22). Also, the design process for the observer, in the latter sections, will be performed on the continuous time model, then applying the time discretization scheme. We refer to (Xia and Manitius, 1993) for another method involving a Diagonally Implicit Runga Kutta technique, which displays very good numerical accuracy when applied to an Euler-Bernoulli beam model.

This section gives a measure of the numerical accuracy of the integration package that is used, by examining the period and energy preservation of the method when applied to the undamped Kirchoff model. For the numerical computations, we take $\gamma = .0001$ and $k = .02$.

The analytical solution to the undamped Kirchoff beam is given by

$$w(x,t) = \sin n\pi x \cos \omega_n t \tag{A.1}$$

with initial conditions

$$w(x,0) = \sin n\pi x, \qquad w_t(x,0) = 0$$

and natural frequencies, ω_n ,

$$\omega_n^2 = \frac{(n\pi)^4}{\gamma(n\pi)^2 + 1}, \qquad n = 1, 2, ...$$

Table 1A gives a comparision of the natural frequencies, ω_n , of the undamped Kirchoff beam, with $\gamma = 0.0001$ and the computed eigenfrequencies for the finite element models with $N = 4, 8, 16, 32, 64$. We see that the first few natural frequencies are quite accurately modelled by the finite element approximation, whereas the high frequencies are not.

Table 2A gives the L_2 and energy norms of the errors between the exact solution , which we take to be the modal solution $w(x,t) = \sin n\pi x \cos \omega_n t$ and the numerical solution. The errors are computed at times $t = 1, 3, 7, 10$ with both the first and third mode excited. The accuracy of the method declines as the higher modes are excited. This is due to the more oscillatory nature of the solution and the inability of the numerical scheme to accurately approximate the more oscillatory systems. The discrete energy norm for the Kirchoff beam is given by

$$\|x_h\|_H = x_h^T \begin{bmatrix} L & 0 \\ 0 & M \end{bmatrix} x_h \; = \; y_h^T \begin{bmatrix} L_m & 0 \\ 0 & I \end{bmatrix} y_h \; = \; \|y_h\|_H \tag{A.2}$$

Table 1A. Table of exact and computed natural frequencies.

Mode N	ω_4	ω_8	ω_{16}	ω_{32}	ω_{64}	ω_n
1	1.3955	1.3951	1.3951	1.3951	1.3951	1.3951
2	5.5941	5.5736	5.5722	5.5721	5.5721	5.5721
3	12.7349	12.5226	12.5076	12.5066	12.5065	12.5065
4	24.5911	22.2455	22.1638	22.1585	22.1581	22.1581
5	38.9116	34.7907	34.4933	34.4730	34.4717	34.4716
6	61.1622	50.2778	49.4412	49.3823	49.3785	49.3783
7	90.8837	68.8660	66.9535	66.8070	66.7974	66.7968
8	109.9543	96.1202	86.9762	86.6577	86.6366	86.6351
9		118.7372	109.4651	108.8375	108.7954	108.7926
10		150.2052	134.3877	133.2441	133.1660	133.1607
11		187.7955	161.7249	159.7713	159.6351	159.6258
12		232.3158	191.4696	188.3116	188.0861	188.0706
13		283.6452	223.6114	218.7580	218.4003	218.3755
14		338.6452	258.0699	251.0054	250.4586	250.4204
15		384.3465	294.2416	284.9525	284.1430	284.0861
16		403.3654	353.8757	320.5029	319.3377	319.2551

Table 2A. Table of energy and $L2$ error norms at $t = 1, 3, 7, 10$ seconds.

N	$\|e(t_1)\|_0$	$\|e(t_2)\|_0$	$\|e(t_3)\|_0$	$\|e(t_4)\|_0$
Mode 1				
4	2.664400E-3	8.1762500E-3	1.322834E-2	1.086700E-2
8	1.901370E-3	1.352502E-4	2.715498E-3	3.177980E-3
16	4.0450400E-4	6.448990E-4	2.441851E-3	3.169890E-5
32	5.954986E-6	1.365655E-5	2.975317E-5	5.525490E-5
Mode 3				
4	2.204498E-0	5.974480E-0	12.000810E-0	13.999552E-0
8	2.6150307E-1	4.3865203E-1	9.318058E-1	1.242059E-0
16	5.586599E-2	5.268059E-2	5.869446E-2	8.999222E-2
32	9.731832E-3	4.159589E-3	2.466896E-2	3.032769E-2
N	$\|e(t_1)\|_H$	$\|e(t_2)\|_H$	$\|e(t_3)\|_H$	$\|e(t_4)\|_H$
Mode 1				
4	2.647000E-3	8.049070E-3	1.321399E-2	1.057080E-2
8	1.901300E-3	1.285039E-4	2.715498E-3	3.177980E-3
16	4.045020E-4	6.448900E-4	2.441850E-3	2.985832E-5
32	5.897427E-6	1.252193E-5	1.262182E-5	5.525490E-5
Mode 3				
4	2.204425E-0	5.973837E-0	11.994815E-0	13.983628E-0
8	2.615021E-1	4.386160E-1	9.931375E-1	1.24077E-0
16	5.586595E-2	5.267914E-2	5.865773E-2	8.98983E-2
32	9.9731831E-3	4.159512E-3	2.466861E-2	3.032657E-2

Table 3A displays the period preservation ability over a long time interval of the LSODE.f program, for $N = 4, 8, 16$. T is the difference between the 1st and 445-th zero, i.e. we allow 222 periods to pass. We take T to be the exact period, based upon the first computed eigenfrequency. $\tilde{T}$ is the difference between the numerical 1st and 445-th zeros. The zeros are computed by linear interpolation. The time step for these results was 0.01.

Table 3A. Table of period preservation for integration package.

γ	N	T (sec)	$\tilde{T}$ (sec)	$T - \tilde{T}$ (sec)
.0001	4	999.584598422	999.8645162116366	2.79917778E-1
.0001	8	999.827710190	999.8676994583235	3.9989210E-2
.0001	16	999.843118771	999.873116416919	2.9997629E-2

Acknowledgements

The author wishes to thank Professor Andrzej Manitius from the Department of Electrical and Computational Engineering at George Mason University for helpful discussions and making the manuscript (Xia and Manitius, 1993) accessible. Also, thanks to Professor Pekka Neittaanmaki for his support and encouragement during my stay at the University of Jyvaskyla in the summer of 1994.

References

Adamian A. and Gibson J.S. (1991): *Approximation theory of linear quadratic Gaussian optimal control of flexible structures.* — SIAM J. Control and Optimization, v.29, pp.1–37 .

Anderson B. and Moore J. (1989): *Optimal Control, Linear Quadratic Methods.* — Prentice-Hall Int., Inc.

Banks H.T., Wang K. and Ito K. (1991): *Exponential stable approximations of weakly damped wave equations.* — Technical Report, ICASE.

Da Prato G., Lasiecka I. and Triggiani R. (1986): *A Direct study of Riccati equations arising in hyperbolic boundary control problems.* — J. Differential Equations, v.64, pp.26–47.

Flandoli F., Lasiecka I. and Triggiani R. (1988): *Algebraic Riccati equations with non-smoothing observations arising in hyperbolic and Euler-Bernoulli boundary control problems.* — Annali di Matematica Pura et. Applicata, v.153, pp.307–382.

Gibson J.S. (1979): *The Riccati integral equations for optimal control problems in Hilbert spaces.* — SIAM J. Control and Optimization, v.17, pp.537-565.

Gibson J.S. (1980): *A note on stabilization of infinite dimensional linear oscillators by compact linear feedback.* — SIAM J. Control and Optimization, v.18, pp.311–316.

Hendrickson E. (1994): *Compensator design for hyperbolic systems with unbounded control operators.* — Technical Report, Dept. of Appl. Math., University of Virginia.

Hendrickson E. and Lasiecka I. (1993): *Numerical approximations and regularizations of Riccati equations arising in hyperbolic dynamics with unbounded control operators.* — Computational Optimization and Applications, v.2, pp.343–390.

Lasiecka I. (1992): *Galerkin approximations of infinite dimensional compensators for flexible structures with unbounded control action.* — Acta Applicandae Mathematicae, v.28, pp.101–133.

Lasiecka I. and Triggiani R. (1991a): *Differential and Algebraic Riccati Equations with Applications to Boundary and Point Control Problems: Continuous and Approximation Theory.* — LNCSI, v.164, New York: Springer Verlag.

Lasiecka I. and Triggiani R. (1991b): *Exact controllability and uniform stabilization of Kirchoff plates with boundary control only on* $\Delta w|_{\Sigma}$ *and homogeneous boundary displacement.* — J. Differential Equations, v.93, pp.62–101.

Russell D.L. (1975): *Decay rates for weakly damped systems in Hilbert spaces obtained via control-theoretic methods.* — J. Differential Equation, v.19, pp.344–370

Triggiani R. (1975): *On the stabilizablity problem in Banach space.* — J. Mathematical Analysis and Applications, v.54, pp.383–403

Triggiani R. (1989): *Lack of uniform stabilization for non-contractive semigroups under compact perturbation.* — Proc. American Mathematical Society, v.105, No.2, pp.375–383.

Xia H. and Manitius A. (1993): *Computational analysis of control and observation of elastic beams.* — Technical Report, No.5–25716, Electrical and Computing Engineering, George Mason University, Virginia.

Received: January 18, 1995